Epitaxial growth of magnesium on Ru(0001)

H. Over,* T. Hertel, and H. Bludau
Fritz-Haber-Institut der Max-Planck-Gesellschaft, Faradayweg 4-6, D-14195 Berlin, Federal Republic of Germany

S. Pflanz
Institut für Kristallographie und Mineralogie, Universität München, Theresienstrasse 41, D-80333 München, Federal Republic of Germany

G. Ertl
Fritz-Haber-Institut der Max-Planck-Gesellschaft, Faradayweg 4-6, D-14195 Berlin, Federal Republic of Germany
(Received 8 February 1993; revised manuscript received 28 April 1993)

The type of growth and the local geometry of magnesium adsorbed on Ru(0001) were investigated by low-energy electron diffraction (LEED), work-function measurements, and thermal-desorption spectroscopy. Despite the large initial dipole moment of 4.5 D the LEED pattern revealed a hexagonal superstructure even at low global Mg coverage ($\theta_{Mg} \geq 0.05$) with local coverage $\theta_{Mg}=0.65$ indicating island growth. In contrast to most alkali-metal/metal systems, where liquidlike adlayers are formed for coverages lower than 0.25, the repulsive dipole-dipole interaction is overcompensated by the overlap of wave functions due to the existence of two valence electrons. During completion of the first monolayer ($\theta_{Mg}=0.75$) the hexagonal superstructure is slightly compressed along the high-symmetry directions of the Ru substrate. This compression is completed when the Mg-Mg distance reaches the corresponding bulk value. Further deposition of Mg leads to a multilayer growth (most likely layer by layer). For such an epitaxially grown, 9-ML thick Mg film on Ru(0001), a LEED structural analysis was performed which revealed Mg bulklike values for the interlayer spacings.

I. INTRODUCTION

The properties of alkali metals on metal surfaces have already been the subject of numerous investigations,[1] in contrast to adsorbed alkaline-earth metals, e.g., Mg. Especially in the low-coverage regime (<1 ML), analysis by low-energy electron diffraction (LEED),[2,3] surface-extended x-ray-absorption fine structure[4] (SEXAFS), scanning tunneling microscopy[5] (STM), and other techniques[6] elucidated the structural properties of alkali metals on metal surfaces. For some systems, somewhat surprising behavior was observed, such as, substitution of substrate atoms by alkali-metal atoms[4(b)] and coverage-dependent adsorption sites,[3(a)] for example.

Alkali-metal adsorbates are considered to be the "simplest" candidates to study the basic mechanisms of chemisorption because of their simple electronic structure (single *s*-valence electron). The adsorption of alkali metals on metals in the submonolayer regime is usually understood in terms of the Langmuir-Gurney model[7] which assumes partial electron transfer from the alkali-metal adatom to the metal substrate to provide an ionic bonding. The partially ionized alkali-metal adatom induces an image charge density at the metal substrate via screening effects. A strongly coverage-dependent dipole moment (depolarization effect) is created which dominates the interaction in the first adsorbate layer by the operation of the dipole-dipole repulsion. This frequently leads to a variety of different ordered structures and usually to the absence of island growth (a prominent counterexample represents the alkali-metal/Al(111) system[8]). If the alkali-metal coverage exceeds 1 ML, the dipole-dipole repulsion is overcompensated by an attractive force which is built up by the overlap of *s*-valence wave functions, thus leading to a metallic character of the alkali-metal layer. During multilayer adsorption, the long-range order is usually destroyed.

Going from the first to the second column in the Periodic Table of elements, the adsorption of alkaline-earth metals on metal substrates is expected to be of a different character since now each adatom provides two valence electrons. To our knowledge, so far only one quantitative structural analysis of such a system has very recently been carried out for Mg/Pd(111) (Ref. 9) by means of x-ray photoelectron diffraction (XPD). It was found that for coverages below 1 ML, Mg atoms occupy fcc sites distributed over two layers, and at higher coverages small oriented clusters consisting of Mg and Pd atoms are formed.

In this paper we report on the system Mg/Ru(0001) which was investigated by thermal desorption spectroscopy (TDS), LEED, and work-function measurements. Among others, a structural analysis by LEED for a 9-ML-thick epitaxially grown Mg overlayer is presented.

II. EXPERIMENT

The experiments were carried out in a UHV chamber (base pressure 7×10^{-11} mbar) equipped with a four-grid LEED optics, facilities for surface cleaning, thermal desorption spectroscopy, Auger electron spectroscopy (AES), and a Kelvin capacitor to measure the work-

function change $\Delta\phi$. The Ru(0001) substrate was cleaned by argon ion sputtering and cycles of oxygen adsorption-desorption. Magnesium was evaporated from a well-outgassed source consisting of a small piece of Mg wire (purity 99.5%) wrapped in Ta foil which could be resistively heated. The typical deposition rate of Mg was about 0.5 ML/min at a sample temperature of 300 K. The coverage was determined by using integrated thermal desorption (TD) spectra in combination with LEED and $\Delta\phi$ measurements; this point will be discussed in more detail following the experimental results.

The contamination of the deposited Mg film by oxygen and CO was estimated to be less than 5% by means of the intensity of the *KLL* oxygen Auger line. Because Mg is very reactive towards oxygen, control experiments were performed in which the Mg-covered surface was purposely exposed to O_2. Small doses of oxygen (about $0.05L$, $1L = 1.3\times10^{-6}$ mbar s) results in a significant overall shift of the Mg TD spectra to higher temperatures. The oxygen contamination of the Mg film could therefore be inspected after the experiments. For measuring periods of less than 1 h, no influence from the residual gas on the TD spectra could be noticed.

We will first describe the change of the LEED pattern with the Mg coverage. Even low Mg coverages ($\theta=0.05$) induced a LEED pattern as shown schematically in Fig. 1 (θ is equal to the amount of adsorbate atoms per substrate first-layer atoms). It can be interpreted as a modulated (5×5) pattern resulting from 16 evenly spaced Mg atoms per unit cell. This hexagonal arrangement of adsorbate atoms leads to a modulation of the spot intensities with "$\frac{4}{5}\times\frac{4}{5}$" periodicity, so that only the corresponding spots and weak double-diffraction spots (small hexagons) around the integer beams became visible. This interpretation of the pattern requires a local coverage of 0.65, thus indicating island growth. Hence, a strong attractive adsorbate-adsorbate interaction is involved. Except for an increase in spot intensities, this superstructure remained unaltered until a total coverage of 0.65 was reached, where obviously the whole surface is covered by domains of this phase. Transforming the lengths of the reciprocal unit mesh vectors into real space (assuming evenly spaced Mg atoms), a lateral Mg-Mg distance of 3.35±0.08 Å can be derived which is expanded by 4% compared to the Mg-Mg bond length in hcp bulk material.

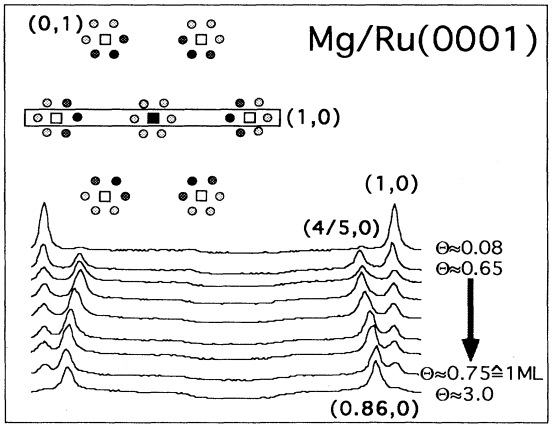

FIG. 1. Schematic picture of the LEED pattern for the submonolayer regime. The gray scales of the circles give a qualitative measure for the relative adsorbate-induced spot intensities. The squares indicate the positions of substrate beams. The LEED profiles as a function of coverage demonstrate the development of the pattern from the (1×1)Ru phase to the (1×1)Mg phase. However, the (0,0)- and first-order fractional beams indicated in the schematic pattern cannot be seen in the profile series due to shadowing by the electron gun.

When the temperature was raised beyond 350 K, the islands of this phase dissolved into a two-dimensional gas ($\theta\leq0.5$). This could be monitored following the temperature dependence of the adsorbate-induced spot intensities. At coverages above $\theta\approx0.5$, this order-disorder transition did not occur prior to desorption due to a rapid increase of the transition temperature. As a peculiarity, an irreversible phase transformation in the coverage interval (0.05–0.25) was observed during the annealing of the Mg film above 550 K. Following the conclusions from an XPD study of the Mg/Pd system,[9] in which intermixing of Mg and Pd was found, this irreversible transition might be correlated with the initial stages of alloy formation. Note that bulk Mg/Ru alloys are known and have already been analyzed in x-ray crystallography.[10]

With prolonged deposition of Mg between $\theta=0.65$ and 0.75, the dominant superstructure spots moved along the high-symmetry directions towards the (1×1) spots (Fig. 1), which is related to a compression of the Mg overlayer in real space. The compression is completed at $\theta=0.75$, resulting in a final Mg-Mg distance around 3.13±0.08 Å close to the metallic Mg-Mg bond length of 3.21 Å. This phase is thus similar to the basal plane of Mg. During the compression phase, the lengths of the reciprocal-lattice vectors are reduced by 7.7%, equivalent to an increase of the local Mg coverage by 16%. Further deposition of Mg beyond $\theta=0.75$ did not affect the geometry of the pattern, but the (1×1) spots and the double-diffraction spots faded out. The only beams in the LEED pattern which survived were the dominant superstructure spots, which in turn provided a (1×1) structure of the Mg film. For higher coverages, the background intensity increased, especially for high energies. In order to determine the geometry of a 9-ML-thick Mg film, *I-V* curves of three beams were measured at normal incidence at a sample temperature of 70 K. The order of the film was slightly improved by a short annealing to 450 K. Similar to this, Wu *et al.* also observed a Mg bulklike hexagonal LEED pattern for 5-ML-thick Mg films on Mo(100) despite pseudomorphic growth in the submonolayer regime.[11]

Figure 2 shows a series of TD spectra taken for various initial Mg coverages. A desorption state (labeled by α) could be observed for small Mg coverages, with its maximum position shifting towards lower temperatures with increasing Mg coverage. Additionally, a small peak can be observed on the high-temperature shoulder of α, similar to TD spectra shown by Malik *et al.*[12]

Before the typical multilayer desorption peaks ap-

peared, a shoulder (labeled by β) on the low-temperature side of peak α became visible, and its onset moved to lower temperatures with increasing Mg coverage. Parallel LEED experiments revealed the formation of the compression phase in the same Mg coverage regime. A comparison of the integrated TD spectrum of the saturated peak β with that of α shows that the Mg coverage was increased by 17% during this stage in good agreement with the value found by LEED (16%). Additionally, the work function revealed a local maximum for the coverage associated with the saturated compression phase. In alkali-metal/metal systems, this observation is assigned to the completion of the first monolayer.[13] It therefore appears to be well founded to define one Mg monolayer just as the coverage of the completed compression phase. Using LEED, we obtained a coverage of $\theta=0.75\pm0.04$. For coverages beyond 1 ML, three multilayer desorption peaks γ, γ', and γ'' can be separated. An evaluation of the corresponding TD integrals shows that each new desorption state evolves when the coverage is close to multiples of the monolayer coverage. Assuming zero-order desorption, an Arrhenius plot of the leading edges yields activation energies for desorption of 146, 136, and 130 kJ/mole for the γ, γ', and γ'' states which are assigned to the second, third, and fourth plus higher layers, respectively. The Mg bulk sublimation energy is 146.4 kJ/mole.[14]

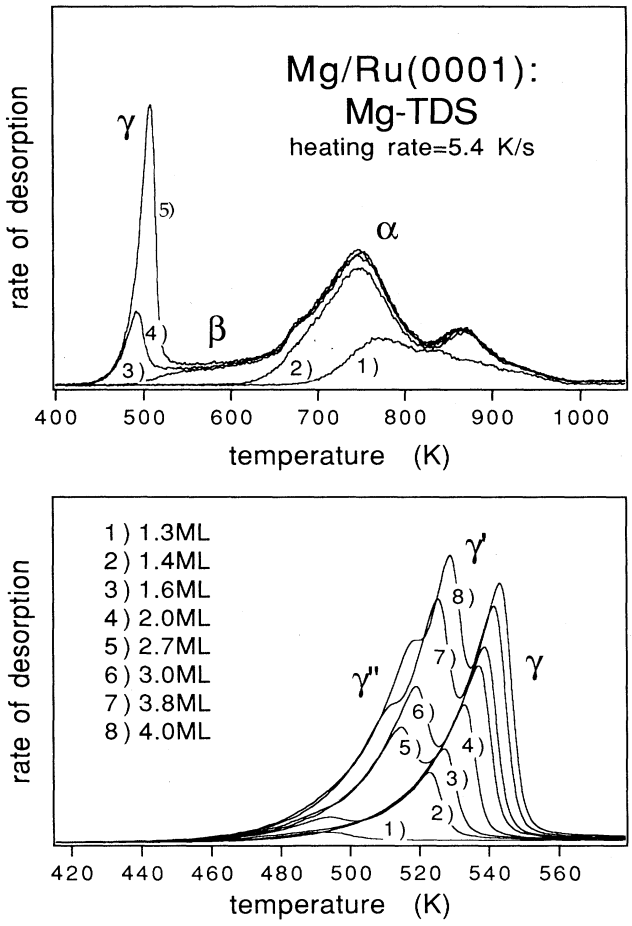

FIG. 2. Series of thermal desorption spectra for different initial coverages of Mg on Ru(0001). In the submonolayer regime (top) the coverage is given with respect to the substrate: (1) $\theta=0.25$, (2) $\theta=0.55$, (3) $\theta=0.71$, (4) $\theta=0.79$, (5) $\theta=0.97$. The multilayer TD spectra (bottom) are identified by their coverage given in physical monolayers (1 ML: $\theta=0.75$).

The variation of the work function $\Delta\phi$ with Mg coverage is reproduced in Fig. 3. For low coverages, the linear decrease of the work function yields a constant initial dipole moment of 4.5 D (1 D$=3.33\times10^{-30}$ Cm). The evaluation was performed by using Helmholtz's formula.[15] In contrast to alkali metals, the ionization energy of Mg (7.65 eV) is significantly larger than the work function of Ru(0001) (5.4 eV); however, the valence orbital of Mg contains two electrons and hence the Gurney model[7(b)] predicts a small charge transfer from Mg to the substrate.

Continuing Mg deposition caused a nonlinear variation of work function for $\theta>0.08$, which at a coverage of 0.19 shows a pronounced minimum followed by a slight increase. At 1 ML ($\theta=0.75$), $\Delta\phi$ passes through a local maximum and finally approaches the Mg bulk value.[16]

Despite the fact that Mg and alkali-metal adsorption are quite different, the $\Delta\phi$ curves look very similar. The nonlinear variation of $\Delta\phi$ in alkali-metal/metal systems (equal to the decrease of the dipole moment) is generally accepted to be caused by the so-called depolarization effect. With increasing coverage, the nearest-neighbor (NN) distance of alkali-metal atoms in the evenly spaced layer become smaller, so that a stronger dipole moment in the opposite direction to the dipole moment of an isolated alkali-metal adatom is induced.

This model cannot be applied to the Mg/Ru(0001) system, since that exhibits island formation for $\theta<0.65$ with constant local coverage. It is suggested that in this case the nonlinear variation of $\Delta\phi$ is due to the fact that Mg atoms in the interior of islands have smaller dipole moments than those located at the boundaries of islands.

The linear decrease of $\Delta\phi$ indicates the coverage range up to which islands consist of a few atoms only. With increasing Mg coverage, the growth of islands is associated

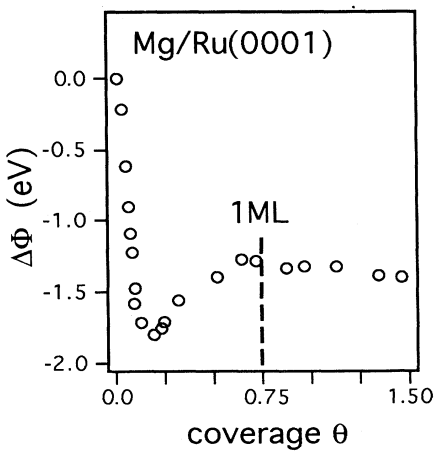

FIG. 3. The work-function change ($\Delta\phi$) vs Mg coverage.

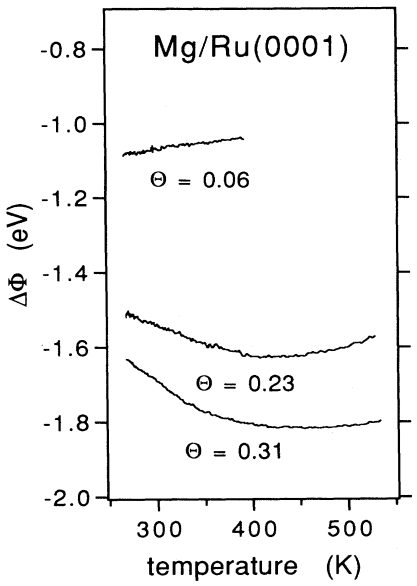

FIG. 4. Temperature dependence of $\Delta\phi$ for three coverages.

with a decreasing ratio of boundary to interior atoms ($\theta_{\text{bound}}/\theta_{\text{interior}}$), thus leading to a nonlinear variation of $\Delta\phi$. The merging of adjacent islands, which decreases the number of boundary atoms and increases the number of interior atoms, is responsible for the minimum and the subsequent increase in $\Delta\phi(\theta)$. This process is completed when the compression phase begins. During the compression, the ordinary depolarization occurs, and $\Delta\phi$ increases further.

This model is supported by the experimentally observed decrease of $\Delta\phi$ as a function of temperature. With increasing temperature, the mean size of the islands should become smaller (the melting process) associated with a larger ratio of $\theta_{\text{bound}}/\theta_{\text{interior}}$. Consequently, the work function decreases with increasing temperature. As shown in Fig. 4, with larger Mg coverage, this effect became more important.

III. LEED ANALYSIS

The technique of LEED has been proven to be well suited to determine both bulk and surface structural properties of ultrathin films.[17] In the following we present a quantitative LEED analysis of a 9-ML-thick Mg film. LEED intensity calculations were performed using a combination of the "layer-doubling method" to describe interlayer scattering and the "layer–Korringa-Kohn-Rostoker (KKR)" approach[18] to treat the multiple scattering within a composite layer. The symmetry of the Mg film was supposed to be $p3m1$ which could be exploited in plane-wave as well as in angular momentum representation;[19] note that both Ru and Mg have an hcp bulk structure and Mg was grown on a Ru(0001) surface. The scattering potential for magnesium was calculated relativistically by overlap from free-atom potentials using Slater's exchange term with Schwarz's optimized α parameter (0.7285);[20] the Mg atoms were arranged in an hcp matrix with lattice constants $a=3.21$ Å and $c=5.21$ Å. The corresponding nine Mg phase shifts were subsequently computed relativistically[21] and spin-averaged. Because no Ru-substrate-derived diffraction spots could be observed in the LEED pattern of the 9-ML-thick Mg film, the multiple scattering via Ru atoms was neglected. The atomic scattering matrices were renormalized for the effects of thermal vibrations (and statistical disorder) using a fixed Debye temperature of 400 K (bulk value[16]) for all Mg layers except the topmost layer where the optimum value turned out be 150 K.

The differences between experimental and calculated I-V curves were quantified by the r_{DE} factor[22] and by Pendry's r factor r_{P},[23] which represent a mean-square deviation of intensities and the Y functions, respectively. In the structural analysis an extended version of a nonlinear least-squares optimization procedure (with respect to the r_{DE} factor and alternatively to the r_{P} factor) for simultaneous refinement of structural and nonstructural parameters was applied.[24,25]

The first step of the analysis was addressed to the determination of the optimum lateral Mg lattice constants supposing an hcp structure. In Fig. 5(a) the r factors as a function of the lattice constant a are shown. The optimum lattice constant a turned out to be 3.16 ± 0.05 Å, while c was 5.20 ± 0.05 Å; in each calculation the first three layer spacings and the real part of the inner potential, as well as the Debye temperature of the first Mg layer, were automatically and simultaneously refined. The two lattice constants found are close to those values obtained for Mg bulk material: $a=3.21$ Å and $c=5.21$ Å.

The sensitivity of this analysis to the first two Mg-layer spacings is displayed in Fig. 5(b) from which a first Mg-layer spacing of 2.64 ± 0.04 Å and a second Mg-layer spacing of 2.58 ± 0.03 Å were derived. Within the error bars both layer spacings are equal to the bulk value of 2.60 Å.

As mentioned above, the Debye temperature of the first Mg layer was also optimized. The resulting influence on the r factors is shown in Fig. 5(c), where small variations of the first two layer spacings were included. Both r factors pass through a pronounced minimum located at 150 K (r_{DE} factor) and 190 K (r_{P} factor), significantly smaller than the bulk value of 400 K.[16] The optimum geometry, however, was still unaffected. A subsequent refinement of the Debye temperatures of Mg atoms situated in deeper layers resulted in a value close to the bulk value. The low Debye temperature in the first layer might be attributed to statistical disorder. Note that the diffraction process occurs on a time interval much smaller than a period of vibration so that dynamic and static disorder are indistinguishable.

In order to tackle the question of the relatively high background found in the corresponding LEED pattern, we performed model calculations simulating a statistical distribution of vacancies in the first three Mg layers as well as statistical occupation of oxygen in a tetrahedral configuration below the Mg top surface layer. A statistical occupation of lattice sites can be introduced in the multiple-scattering formalism using the average-t-matrix

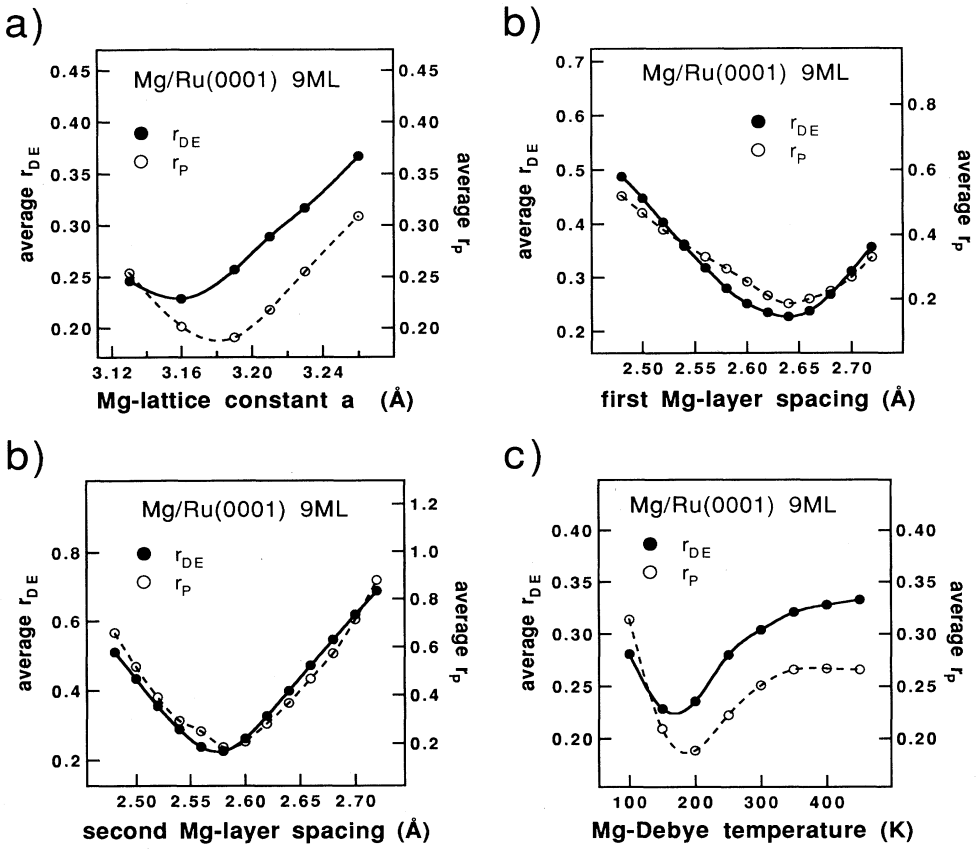

FIG. 5. Dependence of the r factors r_{DE} (solid line) and r_P (dashed line) on (a) the Mg lattice constant a, (b) the first two Mg layer spacings D_1 and D_2, and (c) the Debye temperature of the first Mg layer.

approximation (ATA).[26] The analysis revealed only a very weak sensitivity to the concentration of vacancies in the first three Mg layers so that a density of vacancies smaller than 40% for the first layer, $\leq 20\%$ for the second layer, and $\leq 10\%$ for the third layer cannot be excluded. A small amount of oxygen (3–5 %) located in a tetrahedral configuration, however, led to a significant worsening of the r factors and can therefore clearly be ruled out.

Further model calculations were addressed to the existence of stacking faults. Our analysis gave a clear negative answer. In an XPD study of the system Mg/Pd(111),[9] an interdiffusion of Mg into Pd and alloy formation was observed. A simulation within the framework of the ATA approximation was therefore performed whereby the lattice sites were either occupied by Ru or by Mg atoms with a varying probability related to their concentration. Small amounts of Ru within the first two Mg overlayers resulted in a significant increase of the corresponding r factors, so that intermixing in the first two layers can also be ruled out.

An inspection of the (0,0) beam widths (dependent on the energy of the incident electrons) before and after 9-ML Mg deposition showed the same FWHM (full width at half maximum) oscillations. Since in- and out-of-phase profile widths remained unchanged, the distribution of steps (and all other types of intrinsic defects causing profile broadenings) is similar to that of the bare Ru surface.

This excludes both steps and stacking faults as the predominant defects in the Mg films (as expected for three-dimensional growth or the Stranski-Krastanov mode) and, instead, suggests a layer-by-layer growth that is only disturbed by some "short-scale" defects. Since

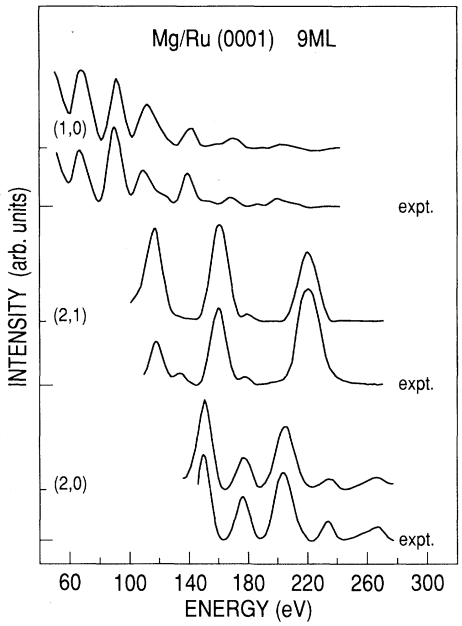

FIG. 6. Comparison of the experimental and calculated best-fit I-V curves for Mg/Ru(0001) 9 ML thick ($r_{DE}=0.15$ and $r_P=0.20$).

substitutional Ru or O atoms in the film can be ruled out by the aforementioned LEED calculation, the relatively high background intensity is attributed to a random distribution of vacancies.

In conclusion, this structural analysis of an epitaxially grown Mg film (9 ML thick) yielded lattice constants $a=3.16$ Å and $c=5.20$ Å very close to those of the Mg bulk material. The first layer spacing was 2.64 ± 0.04 Å, which is expanded by 1.5%, while all other layer spacings equal the bulk values. Statistical distribution of vacancies is very likely responsible for the relatively high background intensity observed in the LEED pattern at higher energies. The low Debye temperature for the first Mg layer supports this conclusion. A comparison of the experimental intensity with spectra calculated for the best-fit geometry is shown in Fig. 6, from which a very good agreement is evident, as quantified by the r factors $r_P=0.15$ and $r_{DE}=0.20$.

IV. DISCUSSION

Frequently, pseudomorphic structure of thin metal films deposited on metal substrates are observed, i.e., below a critical thickness the layer is constrained to match the substrate lattice. For the Mg/Ru(0001) system this growth mode was not observed. This is probably due to the very large mismatch of 18.5%, which would, for pseudomorphic growth, cause too large a strain in the Mg layer. This suggestion is in agreement with theories of epitaxial growth[27] which predict the critical misfit for pseudomorphic growth to be about 7%. If the misfit exceeds 7%, pseudomorphic growth should not take place and misfit dislocations are thought to relieve epitaxial strain. Indeed, we observed incommensurate epitaxial growth; however, there was no indication for misfit dislocation.

The initial growth is rather characterized by hcp island formation in the low-coverage regime ($\theta\leq0.65$). The formation of islands is somewhat surprising because the measured work-function change reveals a relatively high initial dipole moment of 4.5 D. Recalling that alkali metals adsorbed on Ru(0001) generate liquidlike adlayers for $\theta<0.23$, the overlap of wave functions related to the two valence s electrons must be responsible for the attractive interaction, overcompensating the dipole-dipole repulsion in the case of the alkaline-earth metal Mg.

The various stages of Mg film growth on a Ru(0001) surface are sketched schematically in Fig. 7 and can be rationalized as follows.

(a) Adsorbed Mg atoms diffuse across the substrate surface, and nucleation of small islands with hexagonal atomic configurations takes place in which the Mg-Mg separation is 3.35 Å, which exceeds the bulk value by 0.14 Å or 4%.

(b) Beyond $\theta\approx0.1$, the work function no longer decreases linearly with coverage. In contrast to alkali-metal adsorption, this effect is, however, not to be attributed to the growing importance of depolarization associated with continuously shrinking distances between the adparticles, but rather to the varying (i.e., increasing) ratio of Mg atoms located inside the islands and at their perimeters. It is assumed that the perimeter adatoms exhibit a larger dipole moment which is attributed to two effects: These atoms have fewer neighbors and are hence less subject to depolarization; on the other hand, the Smoluchowski effect[28] of atoms at steps (island boundaries) generally causes a decrease of $\Delta\phi$. When islands start to coalesce, the decrease of surface roughness leads to the appearance of the work-function minimum.

(c) At $\theta=0.65$ the growing islands coalesce and cover uniformly the surface. This stage is associated with the completion of the α-state in the thermal desorption spectra. (The origin of the high temperature satellite of this state is still unclear. It might be associated with partial surface alloy formation during heating up of the sample.)

(d) For θ above 0.65, the adlayer is continuously compressed until the Mg-Mg distance reaches the bulk value at $\theta=0.75$. Bonding of the additional Mg atoms within the first layer is still more favorable than the buildup of a second layer, as reflected by the TDS data: The β state builds up as a low-temperature shoulder of the α state (signaling reduced adsorption energy), which is, however, still at distinctly higher temperatures than the γ states. At $\theta=0.75$ the first monolayer is completed, as reflected by the saturation of the β state in TDS, by the work-function maximum, and by the fact that the Mg-Mg distance reaches its bulk value and does not change further.

(e) Beyond $\theta=0.75$ (=1 ML), the work function again decreases slightly and then remains approximately constant. Nevertheless, the second layer is energetically still distinctly different from the third and higher layers, as manifested by the TDS data.

(f) Interestingly, even the third layer still exhibits a distinct TDS peak (γ') before the bulk behavior is reached. The first Mg overlayer already exhibits the lattice constant of the bulk magnesium but is, on the other hand, closely aligned to the high-symmetry directions of the substrate lattice. This situation favors layer-by-layer growth and good epitaxy, as manifested by the high de-

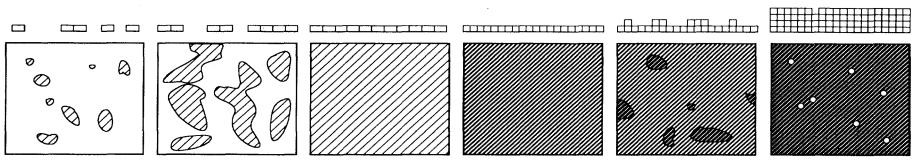

FIG. 7. Schematic illustration of the growth of Mg on Ru(0001): (a) island formation for low coverages ($\theta>0.05$), (b) merging of adjacent islands, (c) uniform Mg film at $\theta=0.65$, (d) completion of the compression phase, (e) growth of a second Mg layer, and (f) several layers with point defects.

gree of crystallinity of the thicker layer whose structure was quantitatively analyzed by LEED.

V. CONCLUSIONS

Using TDS, LEED, and $\Delta\phi$ measurements, the growth of Mg films on a Ru(0001) surface was investigated. During the growth, small islands are formed in the low-coverage regime, which increase in size as further deposition continues until they coalesce to form a nearly continuous film. The lateral Mg-Mg distance is 3.35 ± 0.08 Å. Additional Mg atoms are not adsorbed on top of the first layer to build up a second layer, but are rather incorporated in the first layer, resulting in a uniform compression of this layer. This process is completed when the Mg-Mg distance in the film reaches the corresponding bulk value of 3.21 Å. The evolution of the Mg growth is in line with $\Delta\phi$ measurements. Prolonged deposition causes a layer-by-layer growth which is suggested by the TDS data and LEED observations. A thorough LEED structural analysis was performed for a 9-ML-thick Mg film. The first layer spacing is 2.64 ± 0.04 Å, expanded by 2.5% with respect to Mg bulk, while all other layer spacings equal the bulk value. The relatively high background intensity observed in the LEED pattern for higher energies is attributed to a statistical distribution of vacancies with the highest concentration in the topmost layer.

ACKNOWLEDGMENTS

H.O. gratefully acknowledges fruitful discussions with F. Jona and J. Quinn during a visit to Stony Brook, NY, as well as financial support by the "Deutsche Forschungs-gemeinschaft."

*Present address: University of Wisconsin/Milwaukee, Laboratory for Surface Studies: Physics Building, Milwaukee, WI 53201.

[1] *Physics and Chemistry of Alkali Metal Adsorption,* edited by H. P. Bonzel, A. M. Bradshaw, and G. Ertl, Material Science Monographs (Elsevier, Amsterdam, 1989), Vol. 57.

[2](a) S. A. Lindgren, L. Wallden, J. Rundgren, P. Westrink, and J. Neve, Phys. B **28**, 6707 (1983); (b) C. V. Eggeling, G. Schmidt, G. Besold, L. Hammer, K. Heinz, and K. Mueller, Surf. Sci. **221**, 11 (1989); (c) C. J. Barnes, P. Hu, M. Lindroos, and D. A. King, *ibid.* **251/252**, 561 (1991); (d) D. Fisher, S. Chandavarkar, I. R. Collins, R. D. Diehl, P. Kaukasoina, and M. Lindroos, Phys. Rev. Lett. **68**, 2786 (1992).

[3](a) H. Over, H. Bludau, M. Skottke-Klein, G. Ertl, W. Moritz, and C. T. Campbell, Phys. Rev. B **45**, 8638 (1992); (b) M. Gierer, H. Bludau, T. Hertel, H. Over, W. Moritz, and G. Ertl, Surf. Sci. **279**, L170 (1992); (c) C. Stampfl, M. Scheffler, H. Over, J. Burchhardt, N. M. Nielsen, D. L. Adams, and W. Moritz, Phys. Rev. Lett. **69**, 1532 (1992).

[4](a) G. M. Lamble, R. S. Brooks, D. A. King, and D. Norman, Phys. Rev. Lett. **61**, 1112 (1988); (b) A. Schmalz, S. Aminpirooz, L. Becker, J. Haase, J. Neugbauer, M. Scheffller, D. R. Batchelor, D. L. Adams, and E. Bøgh, *ibid.* **67**, 2163 (1991); (c) S. Aminpirooz, A. Schmalz, L. Becker, N. Pangher, J. Haase, M. M. Nielsen, D. R. Batchelor, E. Bøgh, and D. L. Adams, Phys. Rev. B **46**, 15 594 (1992).

[5](a) R. Schuster, J. V. Barth, G. Ertl, and R. J. Behm, Surf. Sci. Lett. **247**, L229 (1991); (b) Phys. Rev. Lett. **69**, 2547 (1992).

[6](a) M. Kerkar, D. Fisher, D. P. Woodruff, R. G. Jones, R. D. Diehl, P. Kaukasoina, and B. Cowie, Phys. Rev. Lett. **68**, 3204 (1992); (b) J. N. Andersen, M. Quarford, R. Nyholm, J. R. van Acker, and E. Lundgren, Phys. Rev. Lett. **68**, 94 (1992).

[7](a) I. Langmuir and K. H. Kingdon, Phys. Rev. **21**, 380 (1923); (b) R. W. Gurney, *ibid.* **47**, 2798 (1935).

[8] J. N. Anderson, E. Lundgren, R. Nyholm, and M. Quaford (unpublished).

[9] A. Fischer, R. Fasel, J. Osterwalder, A. Krozer, and L. Schlapbach, Phys. Rev. Lett. **70**, 1493 (1993).

[10] L. Westin and L. E. Edshammer, Chem. Scr. **3**, 15 (1973).

[11] M.-C. Wu, J. S. Corneille, J.-W. He, C. A. Estrada, and D. Wayne, J. Vac. Sci. Technol. A **10**, 1467 (1992).

[12] I. J. Malik, J. Hrbek, M.-L. Shek, A. Bzowski, P. Kristof, and T. K. Sham, J. Vac. Sci. Technol. A **10**, 2367 (1992).

[13] N. D. Lang, Phys. Rev. B **4**, 4234 (1971).

[14] *Handbook of Chemistry and Physics,* 67th ed., edited by R. C. Weast, M. J. Astle, and W. H. Beyer (CRC Press, Boca Raton, FL, 1986).

[15] J. Topping, Proc. R. Soc. London, Ser. A **114**, 67 (1927).

[16] C. Kittel, *Introduction to Solid State Physics,* 5th ed. (Wiley, New York, 1976), p. 142.

[17](a) F. Jona and P. M. Marcus, in *Surface Physics and Related Topics,* edited by Fu-Jia Yang, Guang-Jiong Ni, Xun Wang, Kai-Ming Zhang, and Dong Lu (World Scientific, Singapore, 1990), p. 213, and references therein; (b) D. Tian, H. Li, S. C. Wu, J. Quinn, Y. S. Li, F. Jona, and P. M. Marcus, Phys. Rev. B **46**, 7216 (1992); (c) D. Tian, H. Li, J. Jona, and P. M. Marcus, Solid State Commun. **80**, 783 (1991); (d) J. Quinn, Y. S. Li, H. Li, D. Tian, F. Jona, and P. M. Marcus, Phys. Rev. B **43**, 3959 (1991); (e) A. M. Begley, S. K. Kim, J. Quinn, F. Jona, H. Over, and P. M. Marcus (unpublished).

[18](a) J. B. Pendry, *Low Energy Electron Diffraction* (Academic, London, 1974); (b) S. Y. Tong and M. A. Van Hove, Phys. Rev. B **16**, 1459 (1977).

[19](a) J. Rundgren and A. Salwen, J. Phys. C **9**, 3701 (1976); (b) W. Moritz, *ibid.* **17**, 353 (1983).

[20] K. Schwarz, Theor. Chim. Acta (Berlin) **34**, 225 (1975).

[21](a) D. A. Liberman, Phys. Rev. **171**, 1 (1968); (b) D. A. Liberman, D. T. Cromer, and J. T. Waber, Comput. Phys. Commun. **2**, 107 (1971).

[22] G. Kleinle, W. Moritz, D. L. Adams, and G. Ertl, Surf. Sci. **219**, L637 (1989).

[23] J. B. Pendry, J. Phys. C **13**, 937 (1980).

[24] G. Kleinle, W. Moritz, and G. Ertl, Surf. Sci. **238**, 119 (1990).

[25](a) W. Moritz, H. Over, G. Kleinle, and G. Ertl, in *The Structure of Surfaces,* edited by M. A. Van Hove, S. Y. Tong, and Xie Xide (Springer, Berlin, 1991), Vol. III, p. 128; (b) H. Over, U. Ketterl, W. Moritz, and G. Ertl, Phys. Rev. B **46**, 15 438 (1992); (c) M. Gierer, H. Over, W. Moritz, and G. Ertl (unpublished).

[26] F. Jona, K. O. Legg, H. D. Shih, D. W. Jepsen, and P. M. Marcus, Phys. Rev. Lett. **40**, 1466 (1978).

[27](a) J. H. van der Merwe, J. Appl. Phys. **34**, 117, 123 (1963); **41**, 4725 (1970); (b) W. A. Jesser, and J. H. van der Merwe, in *Dislocations in Solids,* edited by F. R. N. Nabarro (Elsevier, New York, 1989), p. 423.

[28] R. Smoluchowski, Phys. Rev. **60**, 661 (1941).